Hydrogen and interstitial Mn complexes in $Mn_xGa_{1-x}As$ dilute magnetic semiconductors

2008 J. Phys.: Condens. Matter 20 125215

(http://iopscience.iop.org/0953-8984/20/12/125215)

J. Phys.: Condens. Matter **20** (2008) 125215 (10pp) doi:10.1088/0953-8984/20/12/125215

Hydrogen and interstitial Mn complexes in $Mn_xGa_{1-x}As$ dilute magnetic semiconductors

F Filippone[1], G Mattioli[1,2] and A Amore Bonapasta[1]

[1] Istituto di Struttura della Materia (ISM) del Consiglio Nazionale delle Ricerche, Via Salaria Km 29.5, CP 10, 00016 Monterotondo Stazione, Italy
[2] Dipartimento di Chimica, Universitá degli Studi di Roma 'La Sapienza', Piazzale Aldo Moro 5, 00185 Roma, Italy

E-mail: francesco.filippone@ism.cnr.it

Received 13 December 2007, in final form 4 February 2008
Published 27 February 2008
Online at stacks.iop.org/JPhysCM/20/125215

Abstract

Complexes formed by H and Mn interstitials (Mn_{int}) in $Mn_xGa_{1-x}As$ dilute magnetic semiconductors (DMSs) have been investigated by using first-principles density functional theory (DFT) methods both in gradient corrected spin density and Hubbard U approximations. In agreement with previous results for complexes of H with substitutional Mn (Mn_{Ga}), present results confirm the importance of electron correlation effects, as the Hubbard U treatment weakens the H–Mn bonds even in the H–Mn_{int} complexes. They also indicate that H compensates (without passivating) the Mn_{int} by forming Mn_{int}–H donor–acceptor (D–A) pairs and, then, Mn_{int}–H complexes. In the H–Mn_{int} and H–Mn_{Ga} complexes, the H–Mn D–A interaction is always mediated by a host atom, thus leading to the formation of H–Ga bonds for interstitial Mn and of H–As bonds for substitutional Mn. This implies quite different H vibrational frequencies for the H–Mn_{int} and H–Mn_{Ga} complexes, thus suggesting that H can be used as a *probe* to discriminate between the two Mn forms through vibrational spectroscopy measurements. Finally, a higher stability of the H–Mn_{int} with respect to the H–Mn_{Ga} complexes has been found, which suggests the use of hydrogenation procedures to control the effects of Mn_{int} on the $Mn_xGa_{1-x}As$ properties.

(Some figures in this article are in colour only in the electronic version)

1. Introduction

Dilute magnetic semiconductors (DMSs) have been widely investigated in recent years due to their peculiar ferromagnetic behaviour, which permits magnetic ordering to be combined with the properties of semiconductors in electron-spin based devices [1–5]. In the DMS, ferromagnetism is due primarily to a coupling between local magnetic moments carried by a metal species (e.g. Mn), that is mediated by conduction-band electrons or valence-band holes. In particular, in the case of Mn substituting the Ga cation in GaAs (Mn_{Ga}), Mn yields both localized magnetic moments and itinerant holes. Recently, the effects of the introduction of atomic hydrogen in $Mn_xGa_{1-x}As$ ($x = 0.037$–0.051) DMS have been experimentally investigated [6–8]. Atomic hydrogen has quite interesting effects on the properties of group IV and III–V semiconductors [9]. It behaves indeed as an amphoteric impurity, which can compensate both acceptors and donors [10, 11]. Moreover, hydrogen diffuses and forms complexes with the impurities by significantly changing their chemical properties. This may cause the disappearance of the electronic levels induced by the impurity in the energy gap, thus leading to a full neutralization or passivation of its electronic effects rather than compensation. In the case of hydrogenated (deuterated) $Mn_xGa_{1-x}As$, infrared measurements have assigned observed frequencies to As–H (As–D) local vibrational modes [6, 7]. Magnetization measurements have shown that as-grown ferromagnetic $Mn_xGa_{1-x}As$ films become paramagnetic after hydrogenation [8]. Moreover, electronic transport measurements have indicated that the density of the free holes is significantly reduced by hydrogenation. In a

previous theoretical study, we have addressed the effects of hydrogenation on the $Mn_xGa_{1-x}As$ ($x = 0.03$) properties by investigating the structural, vibrational, electronic and magnetic properties of complexes formed by H and Mn_{Ga} with density functional theory (DFT) methods [12]. The achieved results show that H forms a stable (Mn_{Ga})–H–As complex, where the calculated stretching frequency of H is in a very good agreement with the experiment. Moreover, the formation of such a complex leads to a full passivation of both the electronic and magnetic properties of Mn, which also agrees with the experiment. As a further result, calculations performed both in gradient corrected spin density (σ-GGA) and Hubbard U (σ-GGA + U) approximations show that electron correlation strongly affects the structure of the Mn–H complexes.

In the present study, we extend our previous theoretical investigations to the case of complexes formed by H and Mn interstitials (Mn_{int}) in GaAs. Different considerations have motivated the present work. First, the high concentrations (some per cent) of Mn in the $Mn_xGa_{1-x}As$ DMS favour the formation of interstitial Mn in these materials with significant effects on the MnGaAs properties. This defect behaves indeed as a double donor and can compensate the acceptor Mn_{Ga} as well as form Mn_{int}–Mn_{Ga} complexes, thus affecting the ferromagnetic behaviour of the $Mn_xGa_{1-x}As$ DMS [5, 13–15]. In this regard, we have investigated here the effects of H on the Mn_{int} properties by considering the characteristics of the H–Mn_{int} interaction, the formation of H–Mn_{int} and H–Mn_{int}–Mn_{Ga} complexes and the existence of possible compensation or passivation effects of H on this interstitial impurity. Second, it is quite difficult to get experimental evidence of the presence of Mn_{int} [16] as well as information on its local atomic environment, that is, on the formation of complexes involving Mn_{int}. Thus, the vibrational properties of the H–Mn_{int} have been also investigated and compared with those of the H–Mn_{Ga} complexes, in the view of H as a *viable local probe* to discriminate between the different forms of Mn in MnGaAs through vibrational spectroscopy measurements. Finally, we expect that an understanding of the H effects on the different forms of the Mn impurity can give suggestions for a defect engineering of the MnGaAs DMS based on hydrogenation treatments [17].

2. Methods

The properties of H–Mn complexes in GaAs have been investigated by DFT methods by using first the σ-GGA approximation [18, 19]. Then, we used the σ-GGA + U formalism [20], as implemented with plane-wave basis sets [21, 18], in order to take into account the strong localization of the d states of Mn, poorly described by σ-GGA exchange–correlation functionals. Total energies have been calculated in a supercell approach, by using ultrasoft pseudopotentials [22], plane-wave basis sets, the special-point technique for **k**-space integration, and the PBE [19] exchange–correlation functional. In detail, the (4, 4, 4) **k**-point Monkhorst–Pack mesh for the simple cubic unit cell, a Gaussian smearing of the occupation numbers and plane-wave cut-offs of 25 Ryd for wavefunctions and 150 Ryd for densities have been used. Wavefunctions included in the As pseudopotential are 4s and 4p, while for Mn they are 3s, 3p, 4s, 4p, 3d. The role of Ga 3d electrons in III–V semiconductor properties has been long debated; in the present work we tested the results of a Ga pseudopotential describing 3d, 4s and 4p orbitals against those coming from a 4s–4p-describing one. As we found only negligible changes, we opted for the lighter 4s, 4p pseudopotential. One interstitial Mn atom has been included in 64-atom supercells of GaAs [6, 8, 12]. The estimated lattice constant corresponding to a 64-atom supercell is equal to 21.27 au.

Geometry optimizations have been performed by fully relaxing the positions of all of the atoms of a supercell by minimizing the atomic forces. The spin state of the system has been self-consistently determined during the wavefunction optimization. Total magnetizations have been calculated as the difference between spin up and spin down densities. Vibrational frequencies have been calculated by scanning the H–M bond (M = Ga, Mn) elongation/tightening up to ±6% of the equilibrium values, and fitting the resulting total energy values to a harmonic second-degree potential. The position of electronic levels induced by a defect (i.e. by Mn or H–Mn complexes) with respect to the top of the valence band has been estimated by calculating the corresponding transition energy levels $\epsilon^{n+1/n}$, that is, the Fermi energy values for which the charge of the defect changes from n to $n + 1$. These values have been estimated as in [23, 24], where further details on the theoretical methods can be found. Transition energy values have to be compared with the GaAs energy gap (E_g) estimated here by the $\epsilon^{+1/0}$ transition level relative to a Si_{Ga} donor (a Si substituting a Ga atom) in GaAs, $\epsilon^{+1/0}[Si_{Ga}]$. A Si_{Ga} behaves as a shallow donor, thus, its $\epsilon^{+1/0}$ level should provide a lower bound estimate of the bottom of the conduction band consistent with the transition levels of the interstitials and H complexes considered here [25]. Such a procedure gives a value of 1.55 eV for the GaAs energy gap, in a fortuitous good agreement with the experimental value (1.5191 eV at 0 K) [26].

A careful analysis of the Mn electronic structure has also been performed by calculating difference electron and spin density maps corresponding to a given electronic level; e.g., the electron and spin ↑ density distributions corresponding to the highest occupied electronic level induced by a Mn_{int} in the energy gap have been estimated by $\rho^{lev}_{diff}[Mn_{int}(0/+1)] = \rho[Mn_{int}{}^0] - \rho[Mn_{int}^{+1}]$ and $\rho^{lev}_{diff}[Mn_{int}(0/+1)]\uparrow = \rho[Mn_{int}^0]\uparrow - \rho[Mn_{int}^{+1}]\uparrow$, respectively, where each density is calculated in a 64-atom supercell with the fixed geometry optimized for the neutral Mn_{int}. Total difference electron density maps have been also used to investigate the nature of the H–Mn interaction and possible charge transfer processes. For instance, given the equilibrium geometry of a H–Mn complex, the total difference density ρ^{tot}_{diff}[H–Mn] = ρ[H–Mn] − (ρ[GaAs-sc] + ρ[H] + ρ[Mn]) has been evaluated, where ρ[H–Mn] is the electron density of the supercell containing the H–Mn complex, ρ[GaAs-sc] is the electron density of the same supercell with the GaAs framework only, and ρ[H] and ρ[Mn] are the electron densities of supercells including, respectively, the H or the Mn atom only, located at their previously computed equilibrium positions. In this way, the

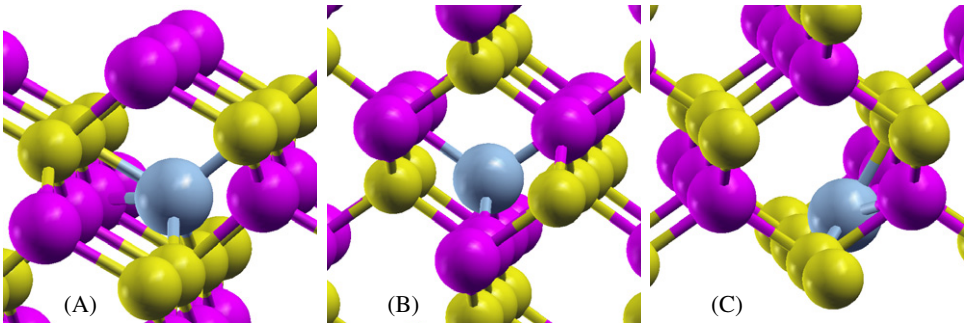

Figure 1. Interstitial sites of Mn in GaAs: (A) tetrahedral site with As neighbours (T-As), (B) the same with Ga neighbours (T-Ga), and (C) hexagonal site (hex). As, Ga, and Mn atoms are represented by light, dark and medium grey (yellow, magenta, and light blue) spheres, respectively.

above sum in round brackets gives the total electron density of the separate and therefore non-interacting parts of the H–Mn complex supercell. Therefore, a $\rho^{\mathrm{tot}}_{\mathrm{diff}}$[H–Mn] map indicates the charge displacements occurring when the interaction between the above parts takes place, positive (negative) values of the density difference in a given region corresponding to an increase (decrease) of electronic charge therein.

3. Results and discussion

The investigation of the H effects on the $\mathrm{Mn_{int}}$ properties has been performed by considering (i) an isolated interstitial $\mathrm{Mn_{int}}$, (ii) a H/$\mathrm{Mn_{int}}$ pair with the two interstitials far from each other, (iii) the H–$\mathrm{Mn_{int}}$ interaction in mono-hydrogen complexes, (iv) the 2H–$\mathrm{Mn_{int}}$ di-hydrogen complexes, and (v) complexes formed by H and a $\mathrm{Mn_{int}}$–$\mathrm{Mn_{Ga}}$ pair. Consequently from the above points, the discussion of results has been organized into five different subsections plus a subsection regarding the stability and vibrational properties of the H–Mn complexes.

3.1. Interstitial Mn

First, the structural properties of a $\mathrm{Mn_{int}}$ have been investigated by locating a Mn atom at different interstitial sites in a GaAs supercell and by fully relaxing the supercell geometry. Three different sites have been considered: a tetrahedral site surrounded by As atoms (T-As), a tetrahedral site surrounded by Ga atoms (T-Ga), and a hexagonal site (hex); see figure 1. At each site, the charge states $-1, 0, +1, +2, +3$ have been considered by subtracting or adding electrons from or to the supercell. Table 1 reports some results for the different Mn sites, i.e. the average atomic distances between Mn and its nearest and next nearest neighbours, the relative total energies, and the total magnetization of the supercell, as given by σ-GGA calculations. No relevant differences have been obtained by performing σ-GGA + U calculations. Transition energy levels for $\mathrm{Mn_{int}}$ located in its stable neutral site, that is, the T-Ga site, are reported in figure 2, first slice. The relative positions of such levels confirm that $\mathrm{Mn_{int}}$ behaves as a double donor, as already suggested in previous studies [4, 5, 13], and may reach the charge state of $+2$ by compensating $\mathrm{Mn_{Ga}}$ atoms. Recall that $\mathrm{Mn_{Ga}}$ behaves as an acceptor; see figure 2, sixth slice, and [12, 27]. Finally, the above results rule out the charge states $+3$ and -1 for a $\mathrm{Mn_{int}}$, which shall not be considered hereafter.

Table 1. Atomic distances, relative total energies, and total magnetization values calculated for an interstitial Mn with different q charges and located at the tetrahedral As (T-As), tetrahedral Ga (T-Ga), and hexagonal (hex) sites are reported in the table. Mn–As and Mn–Ga represent average distances between Mn and its neighbours and next neighbouring atoms. Peculiar distances are reported in parentheses. For each charge state the total energy is relative to the configuration lowest in energy, assumed to be equal to zero.

Site	q	Mn–As (Å)	Mn–Ga (Å)	E (eV)	μ_{T} (μ_{B})
T-As	0	2.52	2.88 (2.32)	0.24	3.00
T-As	+1	2.51	2.93 (2.37)	0.06	4.00
T-As	+2	2.49	2.84 (2.78)	0.00	5.00
T-Ga	0	2.78	2.48	0.00	3.00
T-Ga	+1	2.78	2.52	0.00	4.00
T-Ga	+2	2.78	2.56	0.03	5.00
Hex	0	2.43	2.40	0.23	3.00

As mentioned above, a neutral $\mathrm{Mn_{int}}$ has its stable site at the T-Ga site, $\mathrm{Mn_{(T\text{-}Ga)}}$; see table 1. When positively charged, $+1$ and $+2$, the hex site is not stable (the Mn atom arranges in T sites), while the T-Ga and T-As sites are substantially equivalent in energy. These results can be accounted for by an analysis of the geometrical details reported in table 1. In the neutral case, the average Mn–Ga atomic distance for a $\mathrm{Mn_{(T\text{-}Ga)}}$ is smaller than the average Mn–As distance found for a $\mathrm{Mn_{(T\text{-}As)}}$. This $\mathrm{Mn_{(T\text{-}Ga)}}$–Ga distance increases when going from neutral to positive charge states, thus suggesting that an attractive interaction of a neutral $\mathrm{Mn_{(T\text{-}Ga)}}$ donor with Ga neighbours carrying a partial positive charge weakens when the Mn is positively charged. In the case of neutral $\mathrm{Mn_{(T\text{-}As)}}$, a tendency of Mn to bond to Ga atoms is suggested by a peculiar distance of Mn from one of the Ga next neighbours (the value in parentheses in table 1), shorter than the distances of the $\mathrm{Mn_{(T\text{-}As)}}$ from its As neighbours. When going from neutral to positive charge states, this peculiar Mn–Ga distance also increases, while the average $\mathrm{Mn_{(T\text{-}As)}}$–As distance decreases, because the As neighbours carry a partial negative charge. All together, these results suggest that the $\mathrm{Mn_{int}}$ configurations are mainly affected by the partial charge of the nearest neighbours.

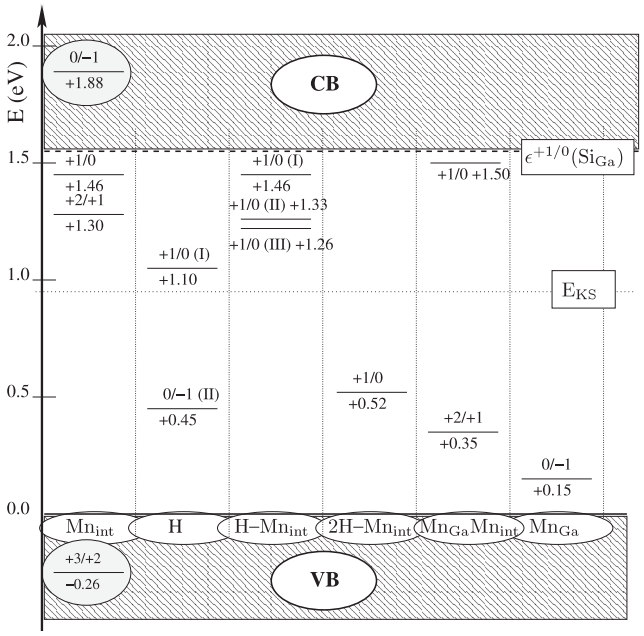

Figure 2. Sketch of transition energy levels in the band gap of GaAs (see text). The energy axis reference is taken on top of the valence band (VB) (i.e. at the Γ point). The conduction band (CB) edge is estimated by the $\epsilon^{+1/0}$[Si$_{Ga}$] transition level for the Si donor defect (dashed bold line). The dotted line indicates the Kohn–Sham eigenvalue gap, E_{KS}. All the values are expressed in eV. The diagram is split into five slices, each relative to one defect or complex. In the first slice there are the transition energy levels relative to interstitial Mn$_{(T\text{-}Ga)}$. In the second slice are reported (I) $\epsilon^{+/0}$[H$_{BC}$] and (II) $\epsilon^{0/-}$[H$_T$]. In the third slice are (I) $\epsilon^{+1/0}$[H–Mn$_{(T\text{-}As)}$], (II) $\epsilon^{+1/0}$[Mn$_{(T\text{-}Ga)}$–Ga–H] and (III) $\epsilon^{+1/0}$[Mn$_{(T\text{-}Ga)}$–H–Ga]. In the fourth slice there is the $\epsilon^{+1/0}$[Mn$_{(T\text{-}Ga)}$–2(Ga–H)]. In the fifth slice there are $\epsilon^{+1/0}$[Mn$_{Ga}$–Mn$_{int}$] and $\epsilon^{+2/+1}$[Mn$_{Ga}$–Mn$_{int}$]. In the sixth slice, $\epsilon^{0/-1}$[Mn$_{Ga}$] from [12] is reported for comparison.

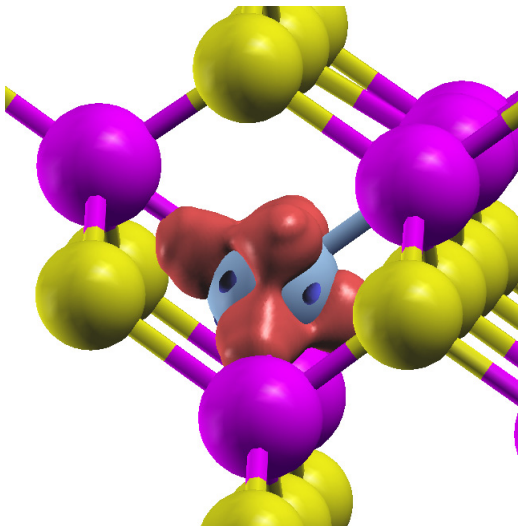

Figure 3. Isosurface of difference electron density distribution for Mn$_{(T\text{-}Ga)}$ (see the text), ρ^{lev}_{diff}[Mn$_{int}$(0/ + 1)]. The isosurface corresponds to a value of 0.0025e/au^3. Medium grey (red) surfaces cover areas where the difference is positive, dark grey (blue) spots cover areas where it is negative. As, Ga, and Mn atoms are represented by light, dark and medium grey (yellow, magenta, and light blue) spheres, respectively.

In fact, the preferred interaction of the neutral Mn$_{int}$ with Ga atoms is balanced, in the case of a positive charge, by an interaction with the negative As neighbours, thus reducing the energy difference between T-As and T-Ga sites.

A qualitative description of the electronic configuration of a Mn$_{int}$ can be achieved by analysing the spin up and spin down electronic eigenvalues and the wavefunction projection on atomic orbitals (not reported here) as well as isosurfaces of the electron and spin density distributions. Recall that the Mn atom starts from a $3d^5 4s^2$ electronic configuration. The analysis of electronic eigenvalues and wavefunctions of a Mn$_{(T\text{-}Ga)}$ and a Mn$_{(T\text{-}As)}$ indicates that in both cases the two highest occupied electronic levels (HOELs), responsible for the Mn$_{int}$ double-donor behaviour, are close in energy, spin↓, and involve mainly two 3d orbitals partially mixed with the 4s orbitals. A pictorial confirmation of this result is given by the electron density distribution corresponding to one of these HOELs, ρ^{lev}_{diff}[Mn$_{int}$(0/ + 1)] = ρ[Mn$_{int}{}^0$] − ρ[Mn$_{int}{}^{+1}$]; see figure 3. The shape of the isosurface in this figure indeed clearly shows the d character of the HOEL electron. A ρ^{lev}_{diff}[Mn$_{int}$(0/ + 1)]↓ (not reported here) substantially identical to that of figure 3 indicates the spin↓ character of the same electron. Almost identical isosurfaces come from the ρ^{lev}_{diff}[Mn$_{int}$(+1/ + 2)] and ρ^{lev}_{diff}[Mn$_{int}$(+1/ + 2)]↓ density distributions for the second HOEL.

The total magnetization of 3 μ_B calculated for the neutral Mn$_{(T\text{-}Ga)}$ can be roughly accounted for by an electronic configuration characterized by three 3d and two 4s spin↑ and the two HOEL spin↓ electrons. Accordingly, the total magnetization increases when the HOEL electrons are removed, as for the positively charged Mn$_{(T\text{-}Ga)}$ (see table 1), or paired with H electrons, as for the H–Mn complexes (see below).

3.2. *H and Mn$_{int}$ donor competition*

The properties of a H/Mn$_{int}$ pair have been investigated by locating these two interstitials far from each other in the same supercell. In detail, a Mn atom has been located at a T-Ga or at a T-As site, while a H atom has been located at a bond centred (BC) site (i.e., the H is located close to the centre of a Ga–As bond) or at a tetrahedral site (T, like the T-Ga site) and a geometry optimization procedure has been performed. In III–V semiconductors H has an amphoteric behaviour [9]: in the case of p-type doping, H behaves as a deep donor by compensating shallow acceptors and forming the H^+ ionized species; in the case of n-type doping, H behaves as a deep acceptor by compensating shallow donors and forming the H^- ionized species. The above BC and T sites are the stable sites of the H^+ (H^+_{BC}) and H^- (H^-_T) species, respectively. Values of transition energy levels for both H$_{BC}$ and H$_T$ are reported in figure 2, second slice. The $\epsilon^{+1/0}$[H$_{BC}$] level is lower in energy than the $\epsilon^{+1/0}$[Mn$_{(T\text{-}Ga)}$] level, that is, a sort of *donor competition* takes place, where the Mn$_{int}$ is a donor stronger than H$_{BC}$. This has relevant consequences, related to the amphoteric character of H, as shown by the fact that the T site is found as the stable

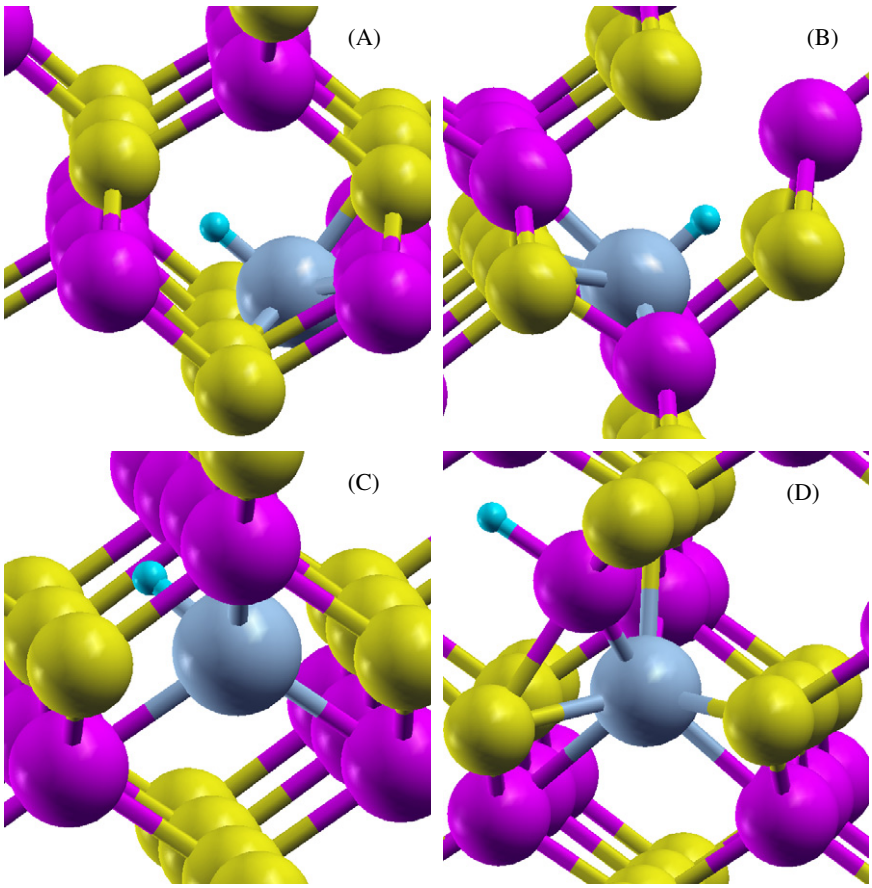

Figure 4. Starting configurations of mono-hydrogen complexes formed with an interstitial Mn located at a hexagonal site (hex) or at a tetrahedral Ga site (T-Ga, see the text): (A) H–$Mn_{(hex)}$; (B) $Mn_{(T\text{-}Ga)}$–H–Ga; (C) H–$Mn_{(T\text{-}Ga)}$–Ga; (D) $Mn_{(T\text{-}Ga)}$–Ga–H. As, Ga, and Mn atoms are represented by light, dark and medium grey (yellow, magenta, and light blue) spheres, respectively. The H atom is represented by a small sphere.

site for H both with $Mn_{(T\text{-}Ga)}$ and $Mn_{(T\text{-}As)}$. That is, in the presence of a Mn_{int}, H behaves as an acceptor by giving rise to $Mn_{int}{}^{+}$–H^{-} donor–acceptor (D–A) pairs. Accordingly, the atomic arrangement around the Mn_{int} turns out to be almost identical to that found for the Mn_{int} with a charge of +1, already seen in table 1. Similarly, two H_T^- species form in the presence of one Mn_{int}, which turns out to have the same atomic arrangement of a Mn_{int} carrying a charge of +2; see table 1. The formation of $Mn_{int}{}^{+}$–H^{-} pairs indicates the existence of a Coulomb driving force favouring the formation of mono-hydrogen H–Mn_{int} complexes; see below. It may be worth noticing that in a supercell containing a Mn_{Ga} acceptor the stable site of H is instead the BC site [12].

3.3. Mono-hydrogen H–Mn_{int} complexes

The properties of neutral mono-hydrogen complexes have been investigated by performing first σ-GGA and then σ-GGA + U calculations on different complex configurations (see figure 4).

The configurations considered are (i) a Mn_{int} located at a hex site and bonded to a H atom which is close to a T-As site, indicated as H–$Mn_{(hex)}$ (see figure 4(a)), (ii) a Mn located midway between a T-Ga and a hex sites in order to permit the insertion of the H atom between the Mn and a Ga neighbour (see the $Mn_{(T\text{-}Ga)}$–H–Ga complex in figure 4(b)), (iii) a Mn located at a T-Ga site with a H atom bonded to Mn and located on the opposite side of a Ga neighbour (see the H–$Mn_{(T\text{-}Ga)}$–Ga complex in figure 4(c)); (iv) in a quite different configuration, H is *bonded to a Ga* neighbouring a $Mn_{(T\text{-}Ga)}$ (see the $Mn_{(T\text{-}Ga)}$–Ga–H complex in figure 4(d)). Similar configurations have been considered for a Mn atom located at a T-As site.

First, we quickly summarize the main differences between the σ-GGA and σ-GGA + U results; then, we discuss in detail the achievements from the latter method. Present σ-GGA and σ-GGA+U results closely parallel those already found in [12]; that is, also when considering an interstitial Mn, in the absence of a beyond-LDA Hubbard-U approach, the Mn 3d levels are too high in energy and therefore tend to over-bind H. In detail, (i) σ-GGA results indicate the H–$Mn_{(T\text{-}As)}$–As, which is characterized by a H–Mn bond, as the most stable complex, while the σ-GGA + U calculations indicate the $Mn_{(T\text{-}Ga)}$–Ga–H of figure 4(D), (ii) in complexes involving H–Mn bonds, σ-GGA H–Mn distances are shorter than σ-GGA + U ones, and (iii) the use of the σ-GGA + U approximation has weaker effects on the complexes where the Mn 3d electrons are less involved, as for the $Mn_{(T\text{-}Ga)}$–Ga–H complex, where H does not bind directly to Mn.

Table 2. Final configuration (final Mn site), atomic distances, relative total energies, and total magnetization values calculated in the σ-GGA + U approximation for neutral and positively charged mono-hydrogen-Mn_{int} complexes. For each charge state the total energy is relative to the configuration lowest in energy, assumed to be equal to zero. The upper and middle parts of the table regard neutral complexes involving a $Mn_{(T\text{-}Ga)}$ and a $Mn_{(T\text{-}As)}$, respectively. The lower part of the table reports results regarding positively charged complexes. Note that Mn was not constrained to stay in the vicinity of any starting configuration.

Complex	Site	H–Mn (Å)	H–X (Å)	X	Mn–Y (Å)	Y	E (eV)	μ_T (μ_B)
$H–Mn_{hex}$	T-Ga	1.81	2.61	As	2.70	Ga	1.18	4.00
$Mn_{(T\text{-}Ga)}$–H–Ga	Hex	1.87	1.81	Ga	2.93	As	0.53	4.00
$H–Mn_{(T\text{-}Ga)}$–Ga	T-Ga	1.79	2.72	As	2.67	Ga	1.17	4.00
$Mn_{(T\text{-}Ga)}$–Ga–H	T-Ga		1.58	Ga	2.40	Ga	0.00	4.00
$Mn_{(T\text{-}As)}$–H–As	Hex	1.81	2.55	Ga	2.76	As	0.62	4.00
$H–Mn_{(T\text{-}As)}$–As	Hex	1.80	2.52	Ga	2.79	As	0.58	4.00
$Mn_{(T\text{-}Ga)}$–H–Ga^+	hex	2.06	1.97	Ga	2.66	As	0.46	5.00
$Mn_{(T\text{-}Ga)}$–Ga–H^+	T-Ga		1.58	Ga	2.67	Ga	0.00	5.00
$H–Mn_{(T\text{-}As)}$–As^+	Hex	1.88	2.73	Ga	2.58	As	0.37	5.00

Regarding the σ-GGA + U results, the final configuration of each H–Mn complex (i.e. the final site of Mn), as given by the geometry optimization procedure, is reported in table 2 together with the corresponding relative total energy and total magnetization values. Table 2 also reports geometrical details of the H–Mn complexes, which include the H–Mn distance and the X–H and Mn–Y distances in a X–H–Mn–Y atomic arrangement, where all of the atoms are located along the same axis and X and Y represent a Ga or As neighbour of H and Mn, respectively.

The mono-hydrogen complexes with the lowest energies, that is, the $H–Mn_{(T\text{-}As)}$–As, the $Mn_{(T\text{-}Ga)}$–Ga–H, and the $Mn_{(T\text{-}Ga)}$–H–Ga complexes, have been also investigated in their positively charged state; see table 2. The corresponding $\epsilon^{+1/0}$ transition levels are reported in figure 2, third slice. Such levels, higher than the corresponding one for H, show that these complexes (i) still have a donor character and (ii) should behave as donors stronger than the H donor. The latter property is confirmed by calculations including the above complexes and a further H atom in the same supercell, where such an atom assumes once more the configuration typical of the H_T^{-1} ionized acceptor. A Coulomb driving force may therefore favour the bonding of a second H atom to mono-hydrogen complexes.

In the stable $Mn_{(T\text{-}Ga)}$–Ga–H complex, the Mn–Ga distance increases from 2.40 to 2.67 Å when going from the neutral to the 1+ charge state. A comparison of this distance with the Mn–Ga distances estimated for a $Mn_{(T\text{-}Ga)}$ in different charge states, see table 1, shows that the local atomic arrangement of Mn in the $Mn_{(T\text{-}Ga)}$–Ga–H^{+1} complex is similar to that found for a $Mn^{+2}_{(T\text{-}Ga)}$. This suggests that in the neutral complex the two HOEL electrons of Mn are involved in the compensation of H and in the Mn–Ga interaction, respectively, while, in the positively charged complex, an electron is lost by the Mn atom, thus accounting for the above Mn–Ga distance increase and the geometrical similarity with the $Mn^{+2}_{(T\text{-}Ga)}$. The occurrence of a H–Mn charge transfer in the neutral complex is confirmed by the difference density distributions ρ^{tot}_{diff}[$Mn_{(T\text{-}Ga)}$–Ga–H] sketched in figures 5(A) and (B). These figures show that a displacement of electronic charge from Mn and from the involved Ga atom to H occurs when the interaction between these atoms is ideally *switched on*.

All together, the above results suggest a quite simple model, which accounts for the stable configurations of the $H–Mn_{int}$ complexes discussed in the present subsection as well as for the structure of the other $H–Mn_{int}$ complexes discussed below. Such a model is based on the following assumptions. (i) Mn_{int} behaves as a double donor. (ii) Mn_{int} is stronger as a donor than H, thus forcing H to an acceptor behaviour. (iii) The donor behaviour and its strength with respect to the H donor persist in complexes where Mn is not fully compensated. Then, Mn or its complexes and atomic H can give rise to D–A pairs, where some electronic charge transfer from Mn to H occurs, e.g., $Mn^{+\delta}$–$H^{-\delta}$ pairs form. (iv) $H^{-\delta}$ ions diffuse and approach $Mn^{+\delta}$ (present in the form of isolated impurity or in a complex), but they do not bind directly to Mn. They form instead complexes whose structure is dominated by the Mn–H D–A interaction and by the interaction of the partially charged $H^{-\delta}$ with a partially positive Ga neighbouring the Mn_{int}. In the proposed model, the H–Mn donor–acceptor interaction is therefore always mediated by a host atom, e.g. the Ga atom in the above $Mn_{(T\text{-}Ga)}$–Ga–H complex.

3.4. Di-hydrogen (2H)–Mn_{int} complexes

Different di-hydrogen configurations have been investigated in the σ-GGA + U approximation by locating a second H atom in different interstitial sites close to the stable $Mn_{(T\text{-}Ga)}$–Ga–H mono-hydrogen complex. Among these, the complex lowest in energy is characterized by a second H atom bonded to a Ga atom neighbouring the Mn atom, in a configuration quite similar to that realized by the first H atom; see figures 5(C) and (D).

This result is consistent with the model proposed above to account for the $H–Mn_{int}$ interaction. In fact, a negative $H^{-\delta}$ ion, attracted by the positively charged $Mn_{(T\text{-}Ga)}$–Ga–H^+ complex, does not bind to Mn, preferring a bond to a Ga neighbouring Mn. Thus, the H–Mn D–A interaction is mediated once more by a Ga atom. In the resulting $Mn_{(T\text{-}Ga)}$–2(Ga–H) complex, both the H–Ga bonds are 1.60 Å long, while the two Mn–Ga bonds are 2.81 Å and 2.74 Å long, respectively. These Mn–Ga distances, larger than the corresponding distance in the $Mn_{(T\text{-}Ga)}$–Ga–H mono-hydrogen complex, confirm that

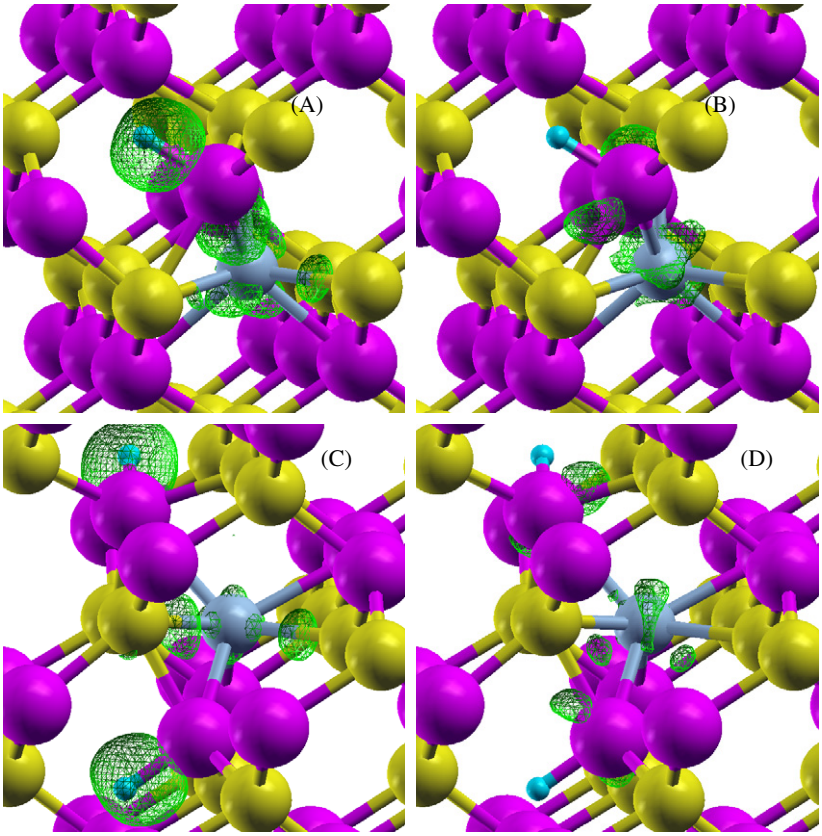

Figure 5. Isosurfaces of the total *difference* electron density estimated for the $Mn_{(T\text{-}Ga)}$–Ga–H complex, $\rho^{tot}_{diff}[Mn_{(T\text{-}Ga)}\text{–Ga–H}]$, are given in (A) and (B). For the $Mn_{(T\text{-}Ga)}$–2(Ga–H) complex, isosurfaces of the $\rho^{tot}_{diff}[Mn_{(T\text{-}Ga)}\text{–}2(Ga\text{–H})]$ are given in (C) and (D), see the text. (A) and (C) show regions where the difference is positive. (B) and (D) show regions where the difference is negative. All of the isosurfaces correspond to a value of $0.005e/au^3$. As, Ga, and Mn atoms are represented by light, dark and medium grey (yellow, magenta, and light blue) spheres, respectively. The H atom is represented by a small sphere. The Mn atomic radius has been reduced in this figure for better displaying the isosurfaces.

the two HOEL electrons of Mn are both involved in the compensation of the two H atoms, thus weakening the Mn–Ga bonding interaction. Accordingly, in the positively charged $Mn_{(T\text{-}Ga)}\text{–}2(Ga\text{–H})^{+1}$ complex, the Mn–Ga distances do not change, the two electrons of Mn being involved in the compensation of the two H atoms. Finally, the isosurfaces of the $\rho^{tot}_{diff}[Mn_{(T\text{-}Ga)}\text{–}2(Ga\text{–H})]$ difference density distributions, sketched in figures 5(C) and (D), parallel those found for the $Mn_{(T\text{-}Ga)}$–Ga–H complex by showing a displacement of electronic charge from Mn and from the involved Ga atoms to H when the D–A interaction between these atoms is *switched on*. The $\epsilon^{+1/0}$ transition energy level of the above $Mn_{(T\text{-}Ga)}$–2(Ga–H) complex (see figure 2, fourth slice) is lower than our estimated $E_g/2$ value, but still in the energy gap. This indicates that H fully compensates interstitial Mn, but at the same time it does not wipe off the Mn-induced electronic levels from the gap. In agreement with the above picture, a total magnetization of 5 μ_B has been estimated for the $Mn_{(T\text{-}Ga)}$–2(Ga–H) complex.

Recalling the results for substitutional Mn [12] and those from all of the previous discussion, a similarity can be found between the H–Mn_{int} complexes and the (Mn_{Ga})–H–As complexes: in both cases an host atom (i.e., respectively, a Ga or As atom) neighbouring the Mn mediates the donor–acceptor interaction. The symmetry between the two cases is straightforward if we consider that a *negative* H is bonded to a Ga *cation* in the presence of the Mn_{int} *donor*, while a *positive* H is bonded to an As *anion* in the presence of the Mn_{Ga} *acceptor*. Notwithstanding, H has quite different effects on the two Mn forms: it passivates Mn_{Ga} while it only compensates Mn_{int}. On the grounds of previous and present results, we can propose a qualitative explanation of such a result. In the case of substitutional Mn, the hole induced by the acceptor is mainly localized on its neighbouring As atoms [12]. H binds to one of these neighbours, by strongly perturbing the Mn–As interaction through the saturation of an As dangling bond. This leads to the Mn passivation. On the other hand, in the case of interstitial Mn, the HOEL electrons responsible for its donor behaviour are localized on the Mn itself. H binds to a Ga weakly bonded to Mn, thus slightly perturbing the Mn environment, which leads just to a Mn compensation.

3.5. Complexes formed by H with Mn_{int}–Mn_{Ga} pairs

When both the donor Mn_{int} and the acceptor Mn_{Ga} impurities are present in a MnGaAs sample, the former can compensate the latter, thus resulting in the formation of Mn^{+2}_{int}–Mn^{-1}_{Ga} D–A pairs. In this case, a Coulomb driving force may favour the diffusion of Mn_{int} and the formation of Mn_{int}–Mn_{Ga} complexes [13]. The formation of such complexes depends

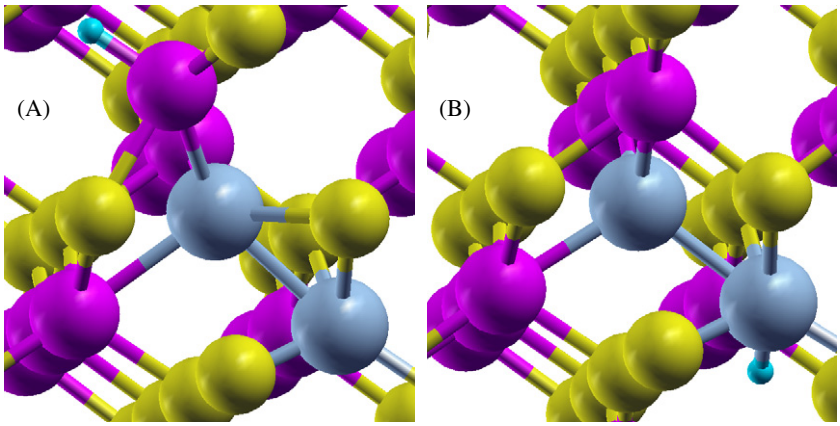

Figure 6. Optimized geometry of the complexes formed by H with a Mn_{int}–Mn_{Ga} pair: (A) H–Ga–$Mn_{(T\text{-}Ga)}$–Mn_{Ga} complex, (B) H–Mn_{Ga}–$Mn_{(T\text{-}Ga)}$ complex. As, Ga, and Mn atoms are represented by light, dark and medium grey (yellow, magenta, and light blue) spheres, respectively. The H atom is represented by a small sphere.

on the experimental procedures used to prepare the MnGaAs samples, which may increase the Mn_{int} concentration as well as enhance its diffusion [4, 13]. The properties of Mn_{int}–Mn_{Ga} and H–(Mn_{int}–Mn_{Ga}) complexes have therefore been investigated here by performing calculations for both their ferromagnetic (FM) and antiferromagnetic (AF) configurations. Regarding the former complexes, the FM $Mn_{(T\text{-}Ga)}$–Mn_{Ga} complex turns out to be the lowest in energy. It is characterized by $Mn_{(T\text{-}Ga)}$–Ga distances between the interstitial and its nearest neighbours equal to 2.56 Å, which are close to the corresponding values estimated for the positively charged $Mn^{+1}_{(T\text{-}Ga)}$, see table 1. This is consistent with a $Mn_{(T\text{-}Ga)}$–Mn_{Ga} D–A interaction and with an attractive interaction between the two impurities in the $Mn_{(T\text{-}Ga)}$–Mn_{Ga} complex. Such an interaction is supported by a dissociation energy of about 1 eV estimated here by assuming breaking the complex into neutral products and by considering the difference between the corresponding total energies.

Given the double-donor character of a Mn_{int}, the structure of a positively charged Mn_{int}–$Mn_{Ga}{}^{+1}$ pair has been investigated too. Also, when charged, the $Mn_{(T\text{-}Ga)}$ –Mn^{+1}_{Ga} pair is lower in energy than the $Mn_{(T\text{-}As)}$–Mn^{+1}_{Ga} one. In the former complex, an increase of the $Mn_{(T\text{-}Ga)}$–Ga distances (2.62 Å) suggests that the missing electron is lost mainly by the donor $Mn_{(T\text{-}Ga)}$. This result agrees with a value of 1.5 eV estimated for the $\epsilon^{+1/0}$ transition level of the same complex (see figure 2, fifth slice). A value of 0.35 eV estimated for the $\epsilon^{+2/+1}$ transition level of the same complex indicates instead that the formation of the $Mn_{(T\text{-}Ga)}$–Mn_{Ga} complex transforms the Mn_{int} from a double to a single donor. Thus, the $Mn_{(T\text{-}Ga)}$–Mn_{Ga} interaction is quite similar to the $Mn_{(T\text{-}Ga)}$–H interaction in the mono-hydrogen complexes, by simply changing the identity of the acceptor, now the substitutional Mn_{Ga} instead of H. All of these results are in the framework of the above proposed model; the $Mn_{(T\text{-}Ga)}$–Mn_{Ga} complex maintains indeed the donor character of the Mn_{int} and is a donor stronger than H. Then, in hydrogenated samples, compensation effects lead to $Mn_{(T\text{-}Ga)}$–Mn^{+1}_{Ga} and H^{-1}_{T} D–A pairs, thus favouring the formation of H–($Mn_{(T\text{-}Ga)}$–Mn_{Ga}) complexes. The structure of these complexes has been investigated by taking into account the stable complex configurations found in the previous study for a H atom interacting with a Mn_{Ga} (see [12]) as well as the results achieved here for the H–$Mn_{(T\text{-}Ga)}$ complexes. Thus, different FM and AF complex configurations have been investigated, where a H atom has been initially located at the following sites: (i) close to a bond centred (BC) site of an As–Mn_{Ga} (i.e., the stable site for a H–Mn_{Ga} complex), which corresponds to an As–H–Mn_{Ga}–$Mn_{(T\text{-}Ga)}$ complex; (ii) bonded to a Ga neighbouring the $Mn_{(T\text{-}Ga)}$, as in the above H–$Mn_{(T\text{-}Ga)}$ complexes, see figure 6(a), which corresponds to a H–Ga–$Mn_{(T\text{-}Ga)}$–Mn_{Ga} complex; (iii) bonded to the Mn_{Ga}, which is referred to as the H–Mn_{Ga}–$Mn_{(T\text{-}Ga)}$ complex (see figure 6(b)); and (iv) bonded to the interstitial Mn in a H–$Mn_{(T\text{-}Ga)}$–Mn_{Ga} configuration. These complexes have been investigated in both their neutral and positively charged forms. The H–Ga–$Mn_{(T\text{-}Ga)}$–Mn_{Ga} AF configuration turns out to be the stable neutral complex formed by H with the Mn_{int}–Mn_{Ga} pair; see figure 6(a). In this complex, the H atom, needed to achieve a full compensation of Mn_{int}, is bonded to a Ga neighbouring the Mn_{int}, thus the Ga atom mediates the H–Mn_{int} interaction, again following the proposed model.

3.6. Stability and vibrational properties of H–Mn_{int} complexes

The stability of the $Mn_{(T\text{-}Ga)}$–Ga–H and $Mn_{(T\text{-}Ga)}$–2(Ga–H) complexes has been estimated by considering their dissociation in neutral species. Total energy differences of 2.3 and 1.6 eV have been estimated for the dissociation reactions

$$Mn_{(T\text{-}Ga)}\text{–Ga–H} \longrightarrow Mn^{0}_{(T\text{-}Ga)} + H^{0}$$

and

$$Mn_{(T\text{-}Ga)}\text{–2(Ga–H)} \longrightarrow Mn_{(T\text{-}Ga)}\text{–Ga–}H^{0} + H^{0},$$

respectively, where H^0 represents a neutral H atom located at its stable site in GaAs [10]. Similarly, a value of 1.7 eV has been estimated for the dissociation energy of the H–Ga–$Mn_{(T\text{-}Ga)}$–Mn_{Ga} complex. A value of 1.8 eV has also been

estimated for the reaction

$$\mathrm{Mn_{(T\text{-}Ga)}}\text{–}\mathrm{Ga}\text{–}\mathrm{H}^{+} \longrightarrow \mathrm{Mn}^{+}_{\mathrm{(T\text{-}Ga)}} + \mathrm{H}^{0}.$$

For comparison, a value of 1.3 eV has been estimated for the dissociation energy calculated for the stable (Mn_{Ga})–H–As complex formed by H and a substitutional Mn_{Ga}. Thus, H–Mn complexes should be more stable when Mn is interstitial.

In the case of the $Mn_xGa_{1-x}As$ DMS, infrared spectroscopy investigations have measured a vibrational frequency of 2143 cm^{-1}, which has been assigned to the H mode of a H–As bond [6]. In our previous theoretical study [12], a value of 2030 cm^{-1} has been estimated for the vibrational frequency of the H–As bond in the (Mn_{Ga})–H–As complex, which favourably compares with the experimental findings. In the case of the H–Mn_{int} complexes investigated here, values of 1633 and 1677 cm^{-1} have been estimated for the stretching frequencies of the two H–Ga bonds in the stable $Mn_{(T\text{-}Ga)}$–2(Ga–H) complex. Values of 1701 and 1720 cm^{-1} are estimated for the stretching frequency of the H–Ga bond in the mono-hydrogen $Mn_{(T\text{-}Ga)}$–Ga–H complex in the neutral and positively charged states, respectively. Finally, values of 1666 and 1593 cm^{-1} have been estimated for the H–Ga and H–Mn bonds formed in the H–Ga–$Mn_{(T\text{-}Ga)}$–Mn_{Ga} and H–Mn_{Ga}–$Mn^{+1}_{(T\text{-}Ga)}$ complexes, respectively. Given the quite different values with respect to H–As frequencies, these results suggest that H may be used as a probe to discriminate between the formation of H complexes with substitutional Mn and interstitial Mn. Moreover, mono-hydrogen and di-hydrogen H–Mn_{int} complexes could be discriminated by exploiting the effects of the D isotope. H can therefore be a precious tool to investigate the presence of interstitial Mn in heavily doped $Mn_xGa_{1-x}As$ DMS through vibrational spectroscopy investigations. Moreover, the above results on the different stability of the H–Mn_{int} and H–Mn_{Ga} complexes suggest that combined hydrogenation procedures, annealing treatments and vibrational spectroscopy measurements in MnGaAs could be exploited to control the effects of Mn_{int}, thus resulting in a sort of hydrogen-based engineering of the material properties. For instance, a careful annealing of a hydrogenated MnGaAs could restore the magnetic activity of the Mn_{Ga} without dissociating the H–Mn_{int} complexes, thus avoiding the damaging effects of Mn_{int} on the MnGaAs magnetic properties.

4. Conclusions

The properties of interstitial Mn (Mn_{int}) and of its mono- and di-hydrogen complexes in GaAs have been investigated here by performing σ-GGA and σ-GGA + U calculations. The latter approach has been used to take into account electron correlation effects on the structure of the H–Mn_{int} complexes. Present results parallel those of a previous study, on complexes formed by H with substitutional Mn (Mn_{Ga}), showing that electron correlation has important effects on H–Mn_{int} complexes too, weakening the H–Mn bonds and favouring complexes where H is bonded to host atoms neighbouring the Mn_{int}. Further results of the present study can be summarized as in the following. (i) The Mn_{int} behaves as a double donor stronger than the H donor, thus forcing H to an acceptor behaviour. This implies a H compensation of Mn_{int}, the formation of Mn_{int}–H donor–acceptor (D–A) pairs, and the binding of diffusing H ions to the charged interstitial Mn. (ii) The structure of the H–Mn complexes is dominated by the D–A interaction, which induces some electronic charge transfer from Mn to H, and by the interaction of the partially charged H with a host atom neighbouring the Mn_{int}. In particular, in all of the investigated H–Mn_{int} complexes, the H–Mn D–A interaction is *always mediated* by a Ga host atom. (iii) A comparison of the structure of the H–Mn_{int} complexes with that of the H–Mn_{Ga} complexes suggests that, independently of the Mn form, the H–Mn interaction is always mediated by a host atom. Even in the case of substitutional Mn_{Ga}, previous theoretical results show indeed that a donor H is bonded to an host atom, i.e., an As atom neighbouring the acceptor Mn_{Ga}. (iv) H passivates Mn_{Ga} while it only compensates Mn_{int}. Present results account for such different effects of H. (v) The occurrence of H–Ga bonds in complexes formed by H and interstitial Mn and of H–As bonds in complexes formed by H and substitutional Mn, predicted by present and previous theoretical results, implies quite different vibrational frequencies for the H local modes in these complexes. H may be used therefore as a *probe* to discriminate the presence of interstitial and substitutional Mn in a MnGaAs DMS through vibrational spectroscopy measurements. Finally, (vi) the H–Mn_{int} complexes are more stable than the H–Mn_{Ga} complexes. Such a different stability suggests that hydrogenation procedures can be exploited to control the effects of Mn_{int} on the MnGaAs properties.

Acknowledgments

We would like to thank M Cococcioni for the many useful discussions about the Hubbard approach. We thank also CINECA and CNR-INFM for the computational support.

References

[1] Ohno H 2002 *Semiconductor Spintronics and Quantum Computation* ed D D Awschalom (Berlin: Springer) p 1
[2] Pearton S J *et al* 2003 *J. Appl. Phys.* **93** 1
[3] Zutic I, Fabian J and Das Sarma S 2004 *Rev. Mod. Phys.* **76** 323
[4] MacDonald A H, Schiffer P and Samarth N 2005 *Nat. Mater.* **4** 195
[5] Jungwirth T *et al* 2006 *Rev. Mod. Phys.* **78** 809
[6] Brandt M S *et al* 2004 *Appl. Phys. Lett.* **84** 2277
[7] Bouanani-Rahbi R *et al* 2003 *Physica* B **340–342** 284
[8] Goennenwein S T B *et al* 2004 *Phys. Rev. Lett.* **92** 227202
[9] See, e.g. Pankove J I and Johnson N M (ed) 1991 *Hydrogen in Semiconductors* (*Semiconductors and Semimetals* vol 34) (New York: Academic)
[10] Pavesi L and Giannozzi P 1992 *Phys. Rev.* B **46** 4621
[11] Amore Bonapasta A and Pavesi L 1996 *Int. J. Quantum Chem.* **57** 823
[12] Filippone F, Amore Bonapasta A and Giannozzi P 2005 *Phys. Rev.* B **72** 121202(R)
[13] Masek J and Maca F 2004 *Phys. Rev.* B **69** 165212
[14] Popovic Z S, Satpathy S and Mitchel W C 2004 *Phys. Rev.* B **70** 161308(R)
[15] Erwin S C and Petukhov A G 2002 *Phys. Rev. Lett.* **89** 227201
[16] Yu K M *et al* 2002 *Phys. Rev.* B **65** 201303(R)
[17] Felici M *et al* 2006 *Adv. Mater.* **18** 1993

[18] Baroni S, Dal Corso A, de Gironcoli S, Giannozzi P, Cavazzoni C, Ballabio G, Scandolo S, Chiarotti G, Focher P, Pasquarello A, Laasonen K, Trave A, Car R, Marzari N and Kokalj A http://www.pwscf.org
[19] Perdew J P, Burke K and Ernzerhof M 1996 *Phys. Rev. Lett.* **77** 3865
[20] Anisimov V I, Aryasetiawan F and Liechtenstein A I 1997 *J. Phys.: Condens. Matter* **9** 767
[21] Cococcioni M and de Gironcoli S 2005 *Phys. Rev.* B **71** 035105
[22] Vanderbilt D 1990 *Phys. Rev.* B **41** 7892
[23] Amore Bonapasta A, Filippone F and Giannozzi P 2003 *Phys. Rev.* B **68** 115202
[24] Van de Walle C G and Neugebauer J 2004 *J. Appl. Phys.* **95** 3851
[25] Amore Bonapasta A, Filippone F and Giannozzi P 2004 *Phys. Rev.* B **69** 115207
[26] Madelung O (ed) 1991 *Data in Science and Technology: Semiconductors* (Berlin: Springer)
[27] Schneider J *et al* 1987 *Phys. Rev. Lett.* **59** 240